INVESTIGATING THE EFFECTS OF OIL PALM ASH IN METAKAOLIN BASED GEOPOLYMER

#ABIDENG HAWA*, DANUPON TONNAYOPAS, WORAPHOT PRACHASAREE*, PICHAI TANEERANANON*

Department of Mining and Materials Engineering, Prince of Songkla University, 90112 Hatyai, Songkhla, Thailand
**Department of Civil Engineering, Prince of Songkla University, 90112 Hatyai, Songkhla, Thailand*

#E-mail: abiding.hawa@gmail.com

Submitted May 15, 2013; accepted November 15, 2013

Keywords: Compressive strength, Geopolymer, Oil palm ash, Drying shrinkage, Expansion

This research reports on the microstructure, compressive strength, drying shrinkage and sulfate expansion of metakaolin (MK) based geopolymers produced by partially replacing MK by oil palm ash (OPA) in proportions of 0 %, 5 %, 10 % and 15 % by weight. The specimens were cured at a temperature of 80°C for 1, 2 and 4 hours, and compressive strength test were conducted at ambient temperature at 2, 6, 24 hours, 7 and 28 day. The testing results revealed that the geopolymer with 5 % OPA gave the highest compressive strength. Scanning electron microscopy (SEM) indicated that the 5 % OPA sample had a dense-compact matrix and less unreacted raw materials which contributed to the higher compressive strength. In the X-ray diffraction (XRD) patterns, the change of the crystalline phase for higher strength was easily detectable compared lower strength.

INTRODUCTION

The term "geopolymer" appears in the fields of materials science and materials engineering. Geopolymers have excellent material properties, including high strength, low shrinkage, acid resistance and excellent durability [1, 2]. The geopolymer process is a chemical reaction between aluminosilicate materials and alkaline solutions under high curing temperature conditions. Over the last several decades, fly ash and metakaolin have been the main raw materials used to produce geopolymer binders. In general, metakaolin is calcined at high temperatures into anhydrous aluminosilicate [3]. Recently, geopolymers have replaced conventional raw materials such as rice husk bark ashes [4].

Previous studies [5-7] have also assessed other mechanical properties such as the compressive strength at more than 1 day. However, in this study was considered in vary high early strength. These other properties are not of primary importance in some application.

Currently, the expansion of oil palm ash from product industries in South East Asia has resulted in an environmental problem for many countries such as Thailand, Malaysia and Indonesia. Oil palm ash (OPA) is a by-product of the processing of palm kernels, palm fibers and palm shells as biomass fuel, which can be used in place of petroleum in electricity generation. In 2011, Thailand produced approximately 10,776,000 tons of oil palm ash [8]. A bunch of fresh palm fruit consists of 21 % palm oil, 6 - 7 % palm kernels, 14 - 15 % palm fibers, 6 - 7 % palm shells, and 23 % empty fruit [9]. Palm kernels, palm fibers, palm shells and empty fruit bunches are all used as biomass fuel. Approximately 5 % OPA by weight of waste materials is produced after fuel combustion [10]. The amount of OPA produced annually in Thailand is approximately 280,000 tons. Currently, OPA is disposed of in landfills, which could lead to environmental problems for the industry and the public. In the present study, geopolymers were prepared, with OPA ratios of 0 %, 5 %, 10 % and 15 %. They were prepared as hot mixtures using sodium silicate and sodium hydroxide as activators before being and heat-cured in an oven at 80°C for 1, 2 or 4 hours. The study aimed to analyze the effect of these parameters on the compressive strength, drying shrinkage and sulfate expansion and used SEM, XRD and FT-IR techniques. Measurements were taken after 2, 6, 24 hours, 7 and 28 days.

EXPERIMENTAL

Materials

The kaolin used in this study was collected from the Narathiwat province of southern Thailand. It was calcined at 750°C for 2 hours and used as Si-Al cementitious material. The chemical composition of the MK was analyzed using X-ray fluorescence (XRF). The physical

properties of the MK are listed in Table 1. Figure 1 depicts the XRD pattern of the MK. The MK showed an apparent amorphous phase (between 17 and 30° 2θ) in its structure with peaks for microcline, quartz and illite. Grinding the raw materials in a ball mill produced small particles (Figure 3).

Table 1. Chemical composition and physical properties of raw materials.

oxides (%)	Metakaolin	OPA
SiO_2	50.30	38.37
Al_2O_3	41.02	1.48
Fe_2O_3	1.05	3.01
CaO	0.33	13.84
TiO_2	1.50	0.21
MgO	–	3.00
K_2O	4.08	14.09
Other	–	5.57
Loss on ignition	1.72	20.43
Specific surface area (m^2/g) BET	13.61	13.06
d_{10} (μm)	1.352	4.321
d_{50} (μm)	6.308	19.305
d_{90} (μm)	88.803	100.109

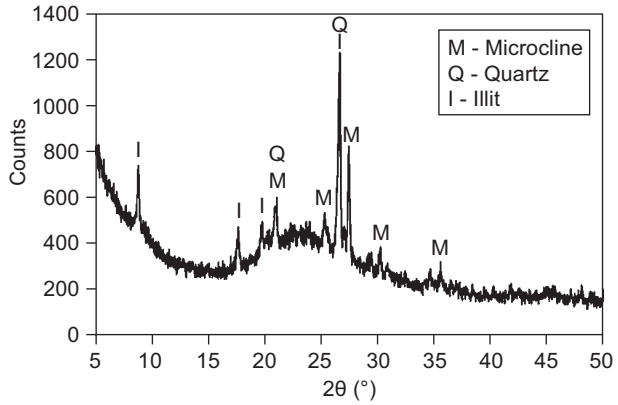

Figure 1. XRD pattern of MK.

OPA was obtained from a palm oil mill in the Krabi province of southern Thailand. It was sieved to remove incompletely combusted fibers. The OPA was ground in a ball mill until the median particle size was approximately 19 μm. The chemical composition and physical properties of the OPA are shown in Table 1. Figure 2 shows the X-ray diffractogram of the OPA, which demonstrates outstanding crystalline phase materials with obvious detectable quantities of crystalline quartz and calcite.

The alkaline solution used was a mixture of sodium hydroxide (NaOH) in flakes of 98 % purity and sodium silicate (Na_2SiO_3). The sodium silicate solution had a composition by weight of 14.14 % Na_2O, 27.67 % SiO_2 and 56.28 % H_2O.

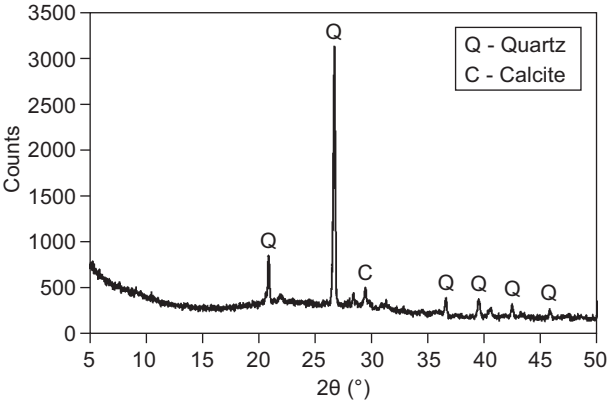

Figure 2. XRD pattern of OPA.

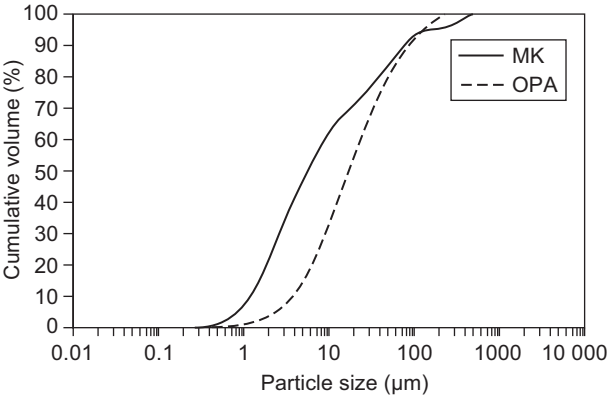

Figure 3. Particle size distribution of raw materials.

Natural river sand was used as the fine aggregate component of the geopolymer mortars. The specific gravity of the river sand was 2.51 and the maximum size was 4.75 mm.

Mixture proportions

Geopolymer mortars were prepared by mixing the raw materials (MK with OPA), river sand and alkaline activators (sodium silicate, sodium hydroxide and water). The sodium silicate and sodium hydroxide were mixed in water and produced an exothermic temperature of 74 ± 2°C. Later, the river sand, MK and OPA, were added to the mixture which reduced the temperature to 48 ± 2°C. Details of the ingredient proportions are shown in Table 2. The slurries were poured into acrylic molds with dimensions of 50 × 50 × 50 mm to form samples for compressive strength testing. The specimens were compacted in accordance with ASTM 109/C 109M [11]. Samples formed in acrylic molds with dimensions of 25 × 25 × 285 mm, compacted in accordance with ASTM C596 [12], were used in tests of drying shrinkage and sulfate expansion. The specimens in acrylic molds were wrapped with polyvinyl to prevent a loss of moisture. All of the specimens were heated in an electric oven at 80°C after casting. After curing for 1, 2 and 4 hours, they

Table 2. Mixture proportions for alkali-activated metakaolin-oil palm ash mortar blends (1000 g).

Sample name	Na_2SiO_3 (g)	NaOH (g)	MK (g)	OPA (g)	Sand (g)	Water (g)	Heat time (h)
Control-1	112	44.8	189.4	–	568.3	85.3	1
O5-1	112	44.8	179.9	9.5	568.3	85.3	
O10-1	112	44.8	170.5	18.9	568.3	85.3	
O15-1	112	44.8	161.0	28.4	568.3	85.3	
Control-2	112	44.8	189.4	–	568.3	85.3	2
O5-2	112	44.8	179.9	9.5	568.3	85.3	
O10-2	112	44.8	170.5	18.9	568.3	85.3	
O15-2	112	44.8	161.0	28.4	568.3	85.3	
Control-4	112	44.8	189.4	–	568.3	85.3	4
O5-4	112	44.8	179.9	9.5	568.3	85.3	
O10-4	112	44.8	170.5	18.9	568.3	85.3	
O15-4	112	44.8	161.0	28.4	568.3	85.3	

were removed from the oven and stored at an ambient temperature of 30 ± 2°C with a relative humidity 70 ± 5 % until they were tested. SEM was conducted using scrap pieces from the specimens subjected to compressive strength tests. XRD and FT-IR were conducted on the geopolymer paste.

Test procedure

Compressive strength tests were conducted on the cast specimens with dimensions of 50 × 50 × 50 mm. After curing for 1, 2 and 4 hours at 80°C, the geopolymer mortars were removed from the acrylic molds and stored at ambient temperature. The samples were tested in accordance with ASTM 109/C 109M [11] at ages of 2, 6, 24 hours, 7 and 28 days.

The drying shrinkage test was performed using a length comparator in accordance with ASTM C490 [13]. The geopolymer mortars were prepared using 1, 2 or 4 hours of curing at 80°C. They were measured during a period of up to 15 weeks.

Sulfate expansion testing of the geopolymer mortars was conducted using prismatic specimens with dimensions of 25 × 25 × 285 mm. The samples were submersed in 5 % Na_2SO_4 and 5 % $MgSO_4$ solutions immediately after being removed from the acrylic molds at 1, 2 and 4 hours. The expansion of the samples was measured each week for 15 weeks using a length comparator in accordance with ASTM C490 [13].

JMS-5800 LV model scanning electron microscope (JEOL, Japan) was performed to verify the microstructure of geopolymer mortars. The samples were divided into small scrap and were used testing techniques of Electron micrograph.

Powder XRD was conducted using an X'Pert MPD X-ray diffractometer (PHILIPS, Netherlands) at angles from 5° to 50° (2Θ) using the clay and rock 0.4 program. The MK, OPA and geopolymer paste were characterized directly. XRD was conducted to identify the dominant crystalline phases and to detect the positions of the peaks.

FT-IR was performed on the geopolymer samples on an EQUINOX 55 spectrometer (Bruker, Germany) using the KBr pellet technique in 4000-400 cm^{-1} range.

RESULT AND DISCUSSION

Compressive strength

The compressive strength testing was focused on the influence of curing time on the compressive strengths of the different mixtures. The compressive strengths of the geopolymer mortars as a function of curing time and amount of MK replacement by OPA are illustrated in Figures 4a to 4d. For all mixtures, long curing times at an elevated temperature were found to accelerate the development of compressive strength after 2 hours (at ambient temperature) better than short curing times. Longer curing may accelerate the degree of geopolymerization because of the formation of long products. However, as Figure 4a shows, the compressive strengths of samples containing only MK after 28 days at ambient temperature were highest for the samples cured for only 1 hour, which is consistent with the findings of Rovnanik [14]. For the specimens cured at 1, 2 and 4 hours and containing 5 % and 10 % OPA, the compressive strength values at 28 days are shown in Figures 4b and 4c, respectively. These results show that the specimens that were cured at 1, 2 and 4 hours did not develop higher long-term compressive strength. The specimens containing 15 % OPA and cured at an elevated temperature for 4 hours had the highest compressive strengths. The influence of curing time on the compressive strengths of specimens cured for 1 and 2 hours was nearly the same at all ages, as illustrated in Figure 4d.

The compressive strengths of the specimens containing various OPA proportions are shown in Figure 5. The effect of OPA addition on compressive strength was slightly less for the control samples cured for 2 hours (at ambient temperature). Beyond this age, the compressive strengths of the 5 % OPA mixtures were higher than

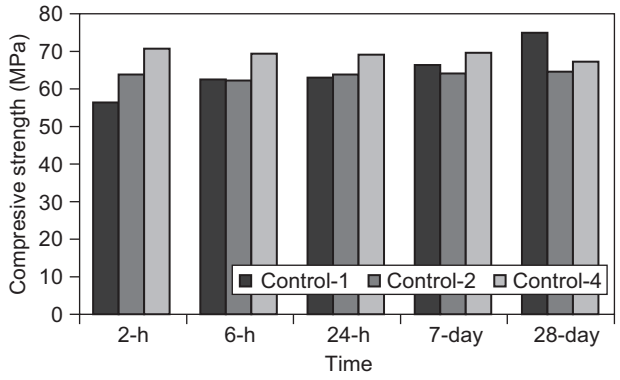

a) Control

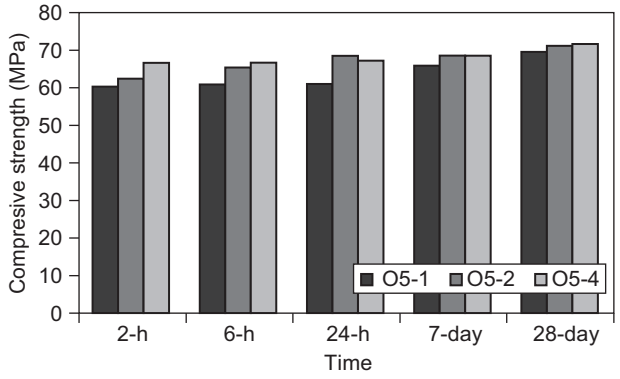

b) 5 % OPA

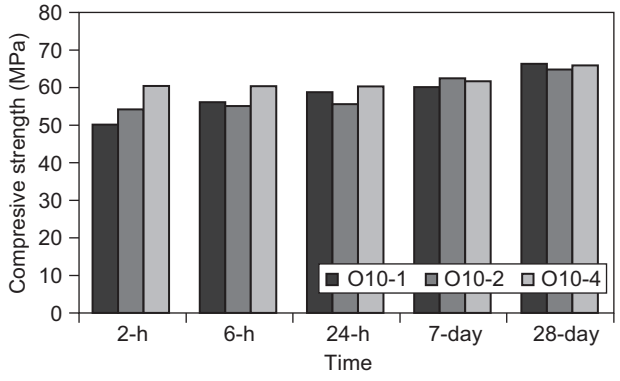

c) 10 % OPA

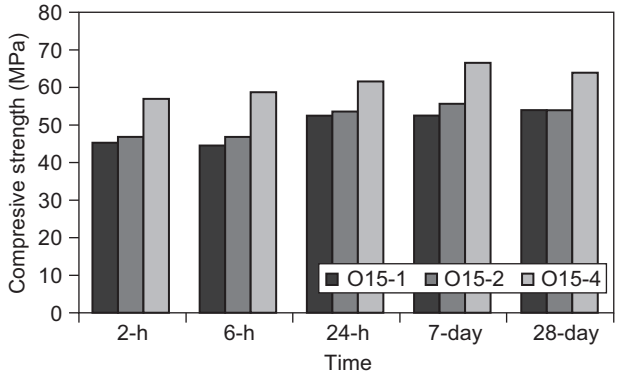

d) 15 % OPA

Figure 4. Compressive strength values of geopolymer mortars Control (a), 5 % OPA (b), 10 % OPA (c) and 15 % OPA (d).

those of the control samples after long curing. In terms of compressive strength, the results suggest that the optimal OPA content is approximately 5 %. It was also observed that these specimens continued to develop compressive strength to an age of 28 days. Because OPA has SiO_2 as its main chemical component, the SiO_2/Al_2O_3 ratio of the geopolymer product is improved by the addition of some OPA. Previous studies [15-17] have reported that different ratios of SiO_2/Al_2O_3 influence the properties of the geopolymer binders. Generally, the geopolymer binder has been prepared using fly ash and metakaolin, in which the ratio of SiO_2/Al_2O_3 varied within a range of 2 to 4. However, adding more OPA beyond the optimal amount decreases compressive strength because the OPA contains CaO. These results are consistent with those of previous studies [18, 19] conducted on fly ash-based geopolymers.

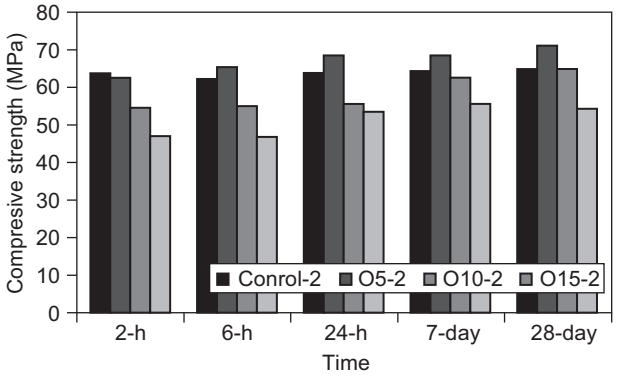

Figure 5. Compressive strength values of geopolymer mortars, control and mortars containing 0 %, 5 %, 10 % and 15 % OPA cured at 80°C for 2 h.

Table 3. Relative compressive strengths of geopolymer mortars.

Sample name	Relative compressive strength values (%)		
	2 h	6 h	24 h
Control-1	100.0	100.0	100.0
O5-1	106.8	97.3	96.6
O10-1	89.1	89.9	93.2
O15-1	80.0	71.3	83.2
Control-2	112.9	99.6	101.0
O5-2	110.8	104.3	108.4
O10-2	99.0	88.0	87.9
O15-2	83.2	74.8	84.7
Control-4	125.2	111.0	109.3
O5-4	117.8	106.5	106.5
O10-4	106.7	96.6	95.7
O15-4	101.0	94.1	97.8

All samples was cured time at elevated temperature and addition of OPA on the compressive strength of samples at ages of 2, 6, 24 hours, 7 and 28 days after mixing. The compressive strengths of the samples ranged from 44.60 to 74.87 MPa. As Table 3 show, the

optimal amount of OPA replacement of MK is up to 5 % by weight of the mixed samples. Replacement of MK by 15 % OPA requires curing for up to 4 hours at an elevated temperature to achieve good long-term strength.

Drying shrinkage

The results of the drying shrinkage tests on the geopolymer mortars are presented in Figures 6a to 6d. The overall result indicated that the drying shrinkage was very low: 0.005 % to 0.050 % and 0.027 % to 0.065 % after 4 and 15 weeks, respectively, at ambient temperature. Higher shrinkage values were obtained for specimens cured for 1 hour at 80°C. As Figure 6a shows, the shrinkage values of the control specimens cured for 1 and 2 hours were similar, while specimens cured for 4 hours shrank less than those cured for 1 and 2 hours. The lower shrinkage of specimens cured longer at an elevated temperature is due to a longer curing at an elevated temperature causes more water to be used in the geopolymerization reaction.. It was also found that the drying shrinkage of specimens cured for 4 hours at an elevated temperature continued for a period of 7 weeks.

Figures 6b to 6d illustrate the drying shrinkage of specimens containing 5 %, 10 %, and15 % OPA, respectively, cured for 1, 2 and 4 hours. All three specimens exhibited similar behavior in terms of longer curing at an elevated temperature decreasing the drying shrinkage. Specimens cured for 2 and 4 hours had similar shrinkage values at all ages, with drying shrinkage decreasing up to an age of 8 weeks. Thereafter, the drying shrinkage values remained constant. However, the drying shrinkage values in the first 8 weeks of specimens cured for 4 hours were less than those of specimens cured for 2 hours. For specimens cured for 1 hour, the drying shrinkage values were much higher at all ages than for specimens cured for 2 hours or 4 hours. In comparison to 1 hour cured specimens, the shrinkage values of 2 and 4 hours cured specimens containing 5 % OPA were -0.044 % and -0.060 %, respectively. The drying shrinkage of specimens cured for 2 and 4 hours were -0.018 % and -0.017 % and -0.039% and -0.027 % after 4 and 15 weeks, respectively. For specimens cured for 1 hour, the drying shrinkage was much higher at all ages than with the longer cure times. Again, longer cure times left less water for evaporation, due to higher extent of geopolymerization reactions that used up water.

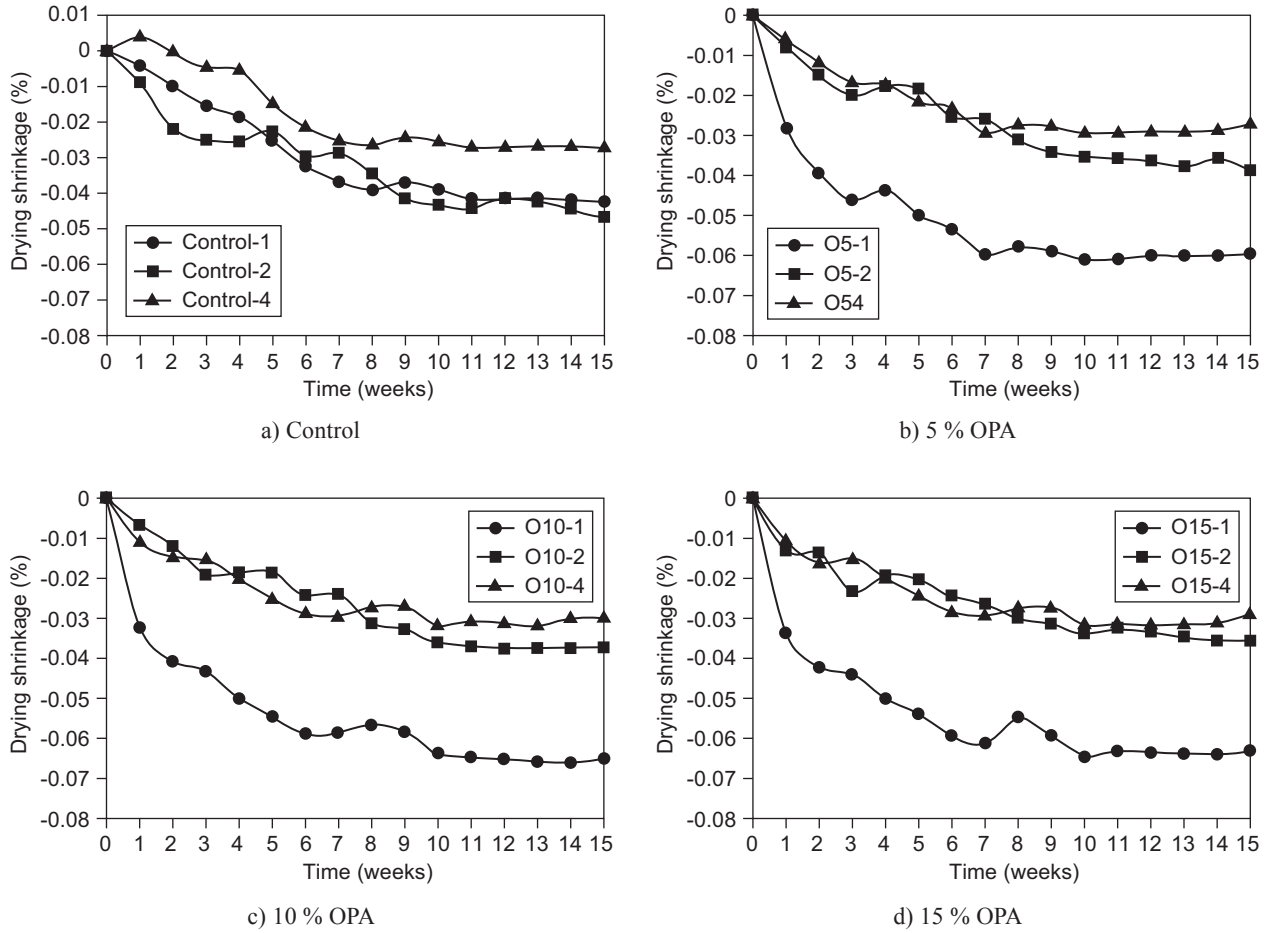

a) Control

b) 5 % OPA

c) 10 % OPA

d) 15 % OPA

Figure 6. Compressive strength values of geopolymer mortars Control (a), 5 % OPA (b), 10 % OPA (c) and 15 % OPA (d).

Sulfate expansion

Figures 7a and 7b illustrate the expansion of geopolymer mortars control at different heat curing time for 1, 2 and 4 hour submersed in solution of 5 % Na_2SiO_4 and 5 % $MgSiO_4$, respectively. The expansion value was similarly significant, while Figures 8a and 8b illustrate the expansion of geopolymer mortars containing 10 % OPA at different curing temperatures and submersed for 1, 2 and 4 hours in solutions of 5 % Na_2SiO_4 and 5 % $MgSiO_4$, respectively. Both Figures illustrate the expansion of the mortars over the range of ages studied. Expansion decreased with decreasing heat curing time. The specimens that were cured at 2 and 4 hours in sodium and magnesium sulfate solutions exhibited similar early and long-term expansion, while the specimens cured for 1 hour exhibited the lowest long-term expansion. Low expansions in sample for 1 hour of exposure may be explained by the feasibility that the samples were more water (longer heat curing causes more water to be used in the geopolymerization reaction).

However, the geopolymer mortars exhibited a different mechanism. Hydration occurs with ordinary Portland cement, but the main geopolymerization product is a product of sodium hydroxide, sodium silicate and raw materials (Si and Al are essential chemical components). Geopolymers submersed in sodium and magnesium sulfate solutions have a more stable cross-linked aluminosilicate polymer structure [1]. It should be noted that the geopolymer mortars in this study had high compressive strength and suppressed sulfate expansion in the presence of sodium and magnesium sulfate solutions.

Scanning electron microscopy (SEM)

SEM results shown in Figure 9 represent typical microstructures of geopolymerization products obtained from this investigation. Comparison of the SEMs of Control-2 and O5-2 specimens revealed that a few unreacted raw materials were coated to some extent with flakes formed on the crust of Control-2 specimens and revealed of the specimens to be nonhomogeneous, whereas in O5-2 specimens, a lower proportion of unreacted raw materials were detected in the samples (see Figure 9b). It was also found that O5-2 samples had high homogeneity in comparison to Control-2 samples.

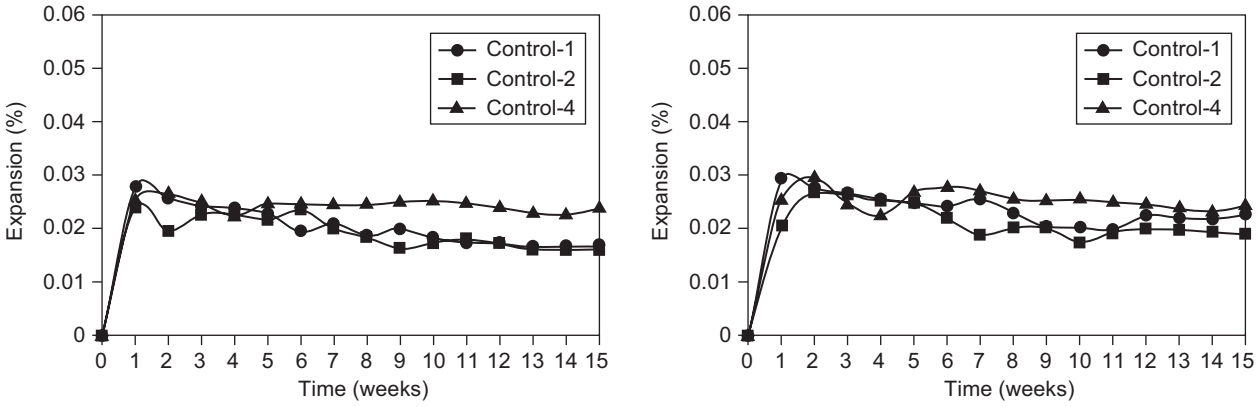

a) Na_2SO_4 b) $MgSO_4$

Figure 7. Expansion values of geopolymer mortars control submerged in sulfate solutions Na_2SO_4 (a) and $MgSO_4$ (b).

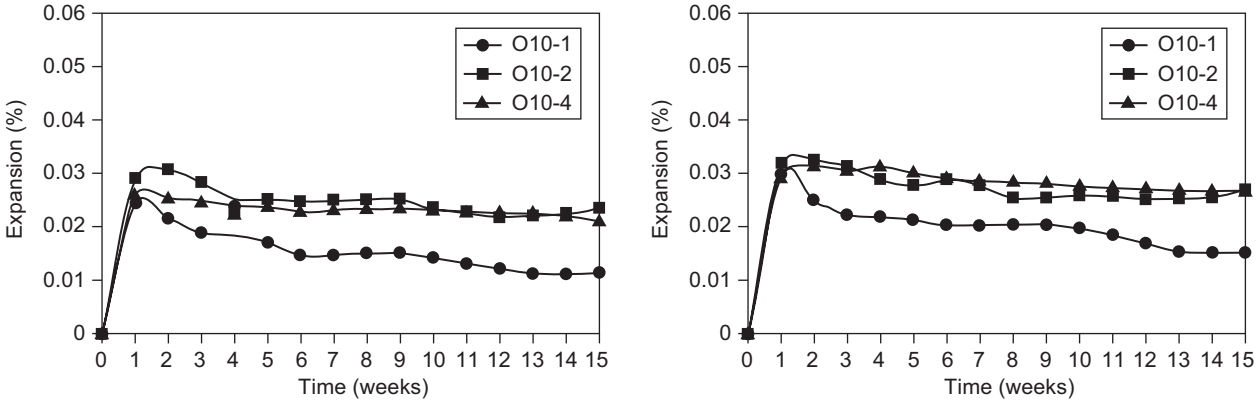

a) Na_2SO_4 b) $MgSO_4$

Figure 8. Expansion values of geopolymer mortars containing 10 % OPA submerged in sulfate solutions Na_2SO_4 (a) and $MgSO_4$ (b).

The compressive strengths of the O5-2 samples were greater than the compressive strengths of the Control-2 samples, as shown in Figure 5.

Figures 10a and 10b specimens showed that a few unreacted raw materials were covered somewhat with flakes formed on crust in O15-1 and O15-2 specimens and showed also that of many porous matrix. Nevertheless, O15-4 (Figure 10c) it was observed that a homogeneous matrix and dense-compact microstructure with less proportion of unreacted raw materials in the samples. This is consistent with the test result are compressive strength in Figure 4d.

X-ray diffraction (XRD)

Figures 11a and 11b are shows the XRD patterns for sample Control and O5 with various heat-curing at 1, 2 and 4 hours. The samples had a similar pattern being mostly amorphous with some crystalline peaks. The XRD pattern for the 4 hours with O5 sample shows that the apparent quartz content was detected most obviously at approximately 21°, 27° and 50° 2θ compared to the samples heat-cured for 1 and 2 hours. This indicates that crystalline phases were detected in the geopolymer samples and that heat-curing at 4 hours produced the highest amount of crystallinity and had a higher compressive strength (see Figure 4). On the other hand, the XRD pattern for 1 hour with Control sample

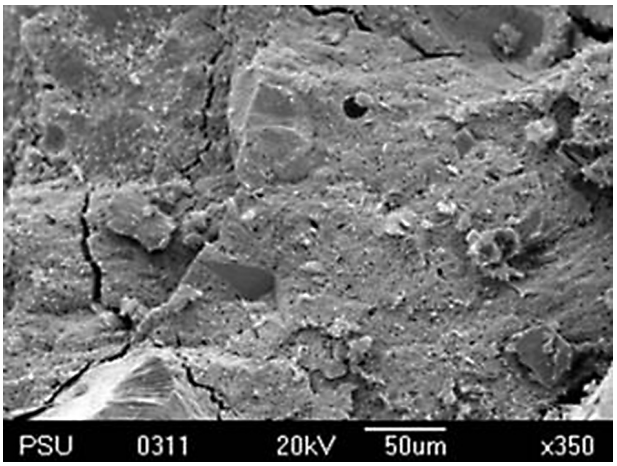

a) Control-2

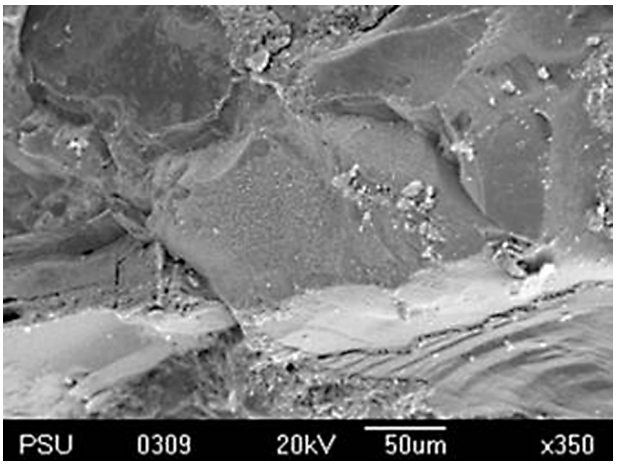

b) O5-2

Figure 9. SEM images of geopolymer mortars cured at 80°C for 2 hours Control-2 (a) and O5-2 (b).

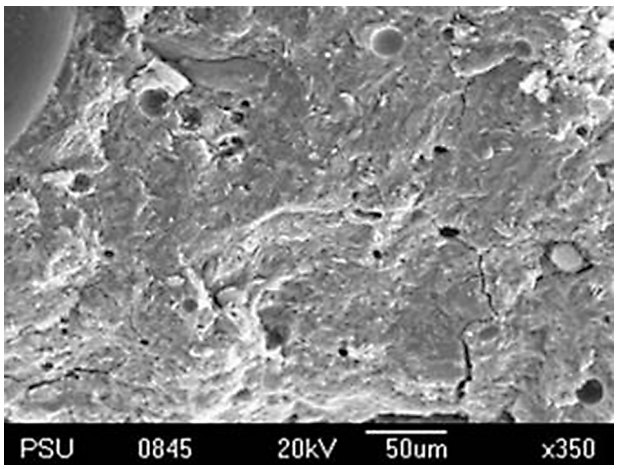

a) O15-1

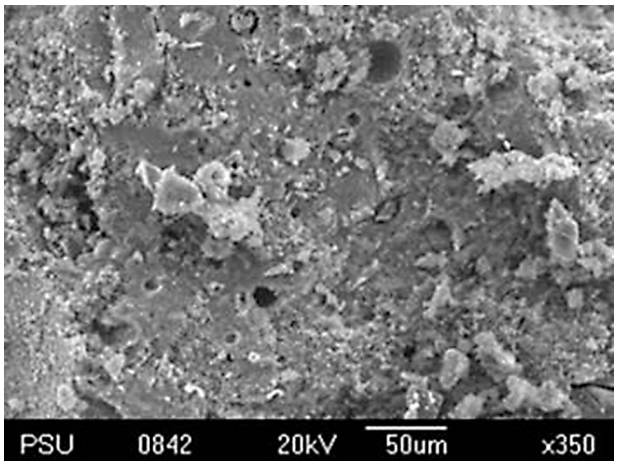

b) O15-2

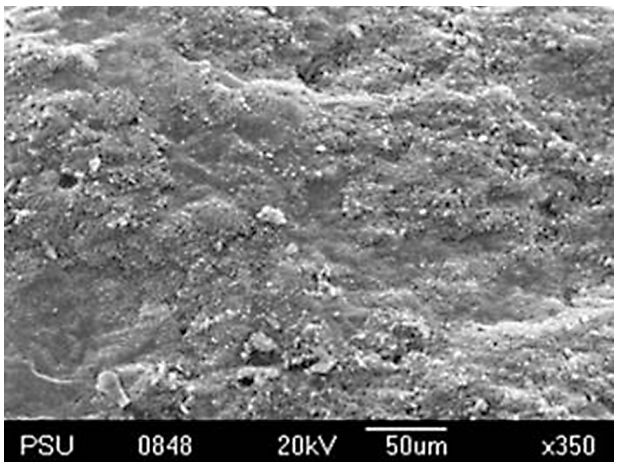

c) O15-4

Figure 10. SEM image of geopolymer mortars cured at 80°C containing 15 % OPA O15-1 (a), O15-2 (b) and O15-4 (c).

was highest amount of crystallinity and had a higher compressive strength (see Figure 4a). Similarly, the trend of high amount of crystallinity and had a higher compressive strength has been found in the previous researcher [7, 18].

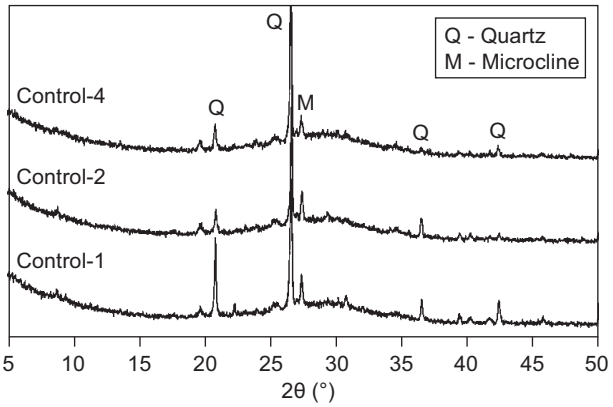

a) Control

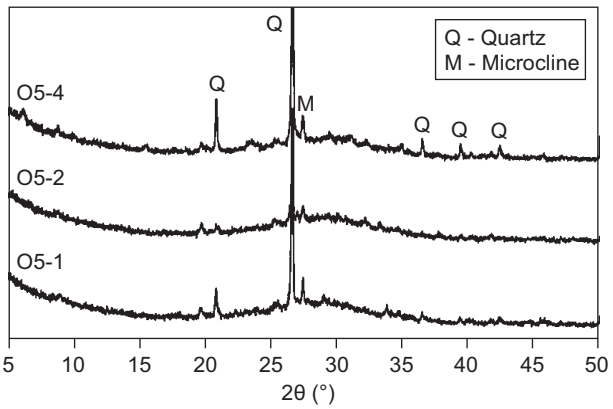

b) 5 % OPA

Figure 11. XRD pattern of geopolymer Control (a) and 5 % OPA (b).

Fourier transform infrared spectrophotometer (FT-IR)

Figure 12 shows the FT-IR spectra for the Control-2 and O5-2 samples with those of MK and OPA for purposes of comparison. The MK spectrum contains wide bands at approximately 1083 and 464 cm^{-1}, reflecting the Si–O vibrations. These major bands are observed at frequencies near to these reported in the literature for this compound [20]. There is also a band at 810 cm^{-1} corresponding to Al–O. For the OPA spectra, the stretching of the Si–O groups alternately bound to the Al–O bonds produces a signal at 1030 cm^{-1} and a band around 789 cm^{-1} indicative of the Al–O or Si–O–Al groups. These major bands have also been reported in the literature [21].

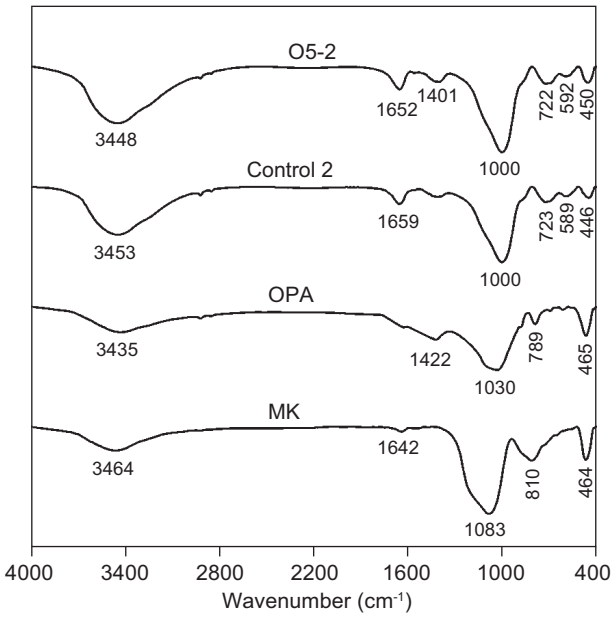

Figure 12. FT-IR spectra of raw materials and the geopolymer samples heat-cured for 2 hours.

The FT-IR spectra of the Control-2 sample (see Figure 12) indicate major bands at approximately 3453, 1659, 1408, 1000, 723, 589 and 446 cm^{-1}. Those at 3453 and 1659 cm^{-1} are formed by the O–H stretching vibration and the H–O–H bending vibration, respectively and these have been previously noted in hydroxyl groups [20]. The main binder system vibration band at approximately 1000 cm^{-1} is attributable to the asymmetric stretching mode of the Si–O–Al bond in the reaction products and this vibration band has also been found in previous research [22]. The main bands in the geopolymers are only a little different from those in the FT-IR spectra of the MK between 450 and 1200 cm^{-1}. It has been previously reported that some raw material is retained in the geopolymerization products [23]. The results of the present study suggest that the composition of the aluminosilicate was formed by the geopolymerization of the MK and/or the OPA and the alkaline activator produces slightly different FT-IR patterns. The effect of the OPA ratio on the nanostructure as shown by the FT-IR spectra in Figure 12 is rather limited. The trend of the FT-IR spectra in previous research has been similarly adopted [24] where it has been reported that difference in the w/b ratio in the gel nanostructure of the fly ash based geopolymer as displayed by the FT-IR spectra is rather limited.

It was observed that the main binder system vibration band occured at approximately 1000 cm^{-1} which can be attributed to the asymmetric stretching mode of the Si–O–Al bond, as shown in Figure 13. However, the compressive strength of the geopolymer mortars produces a trend of lower transmittance (high absorption), which reflects the higher strength of the geopolymer as detected in the FT-IR test.

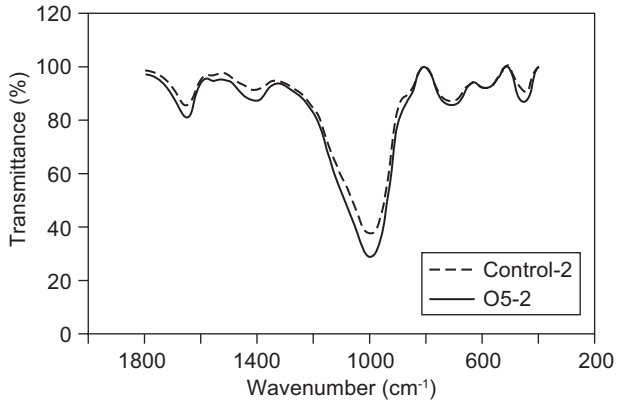

Figure 13. FT-IR spectra of the geopolymer samples.

CONCLUSIONS

This study examined the influence of various mix proportions and ambient curing temperatures for geopolymer mortar specimens and their behavior in terms of linear drying shrinkage and magnesium sulfate and sodium sulfate expansion at different curing times. The following conclusions are drawn:

- Compressive strength values gradually increased with time in the oven at early ages (2 hours at ambient temperature).
- The highest compressive strengths of the MK-based geopolymer mortar mixes studied were obtained for mixes containing 5 % OPA for all curing times considered.
- For geopolymer mortars containing OPA, increasing curing time at an elevated temperature decreased drying shrinkage, potentially due to the well-developed strength.
- Submersing geopolymer mortars in sodium and magnesium solutions and curing them for 1 hour at an elevated temperature can reduce expansion.

The increased compressive strength was attributable to the structure of the geopolymer samples which had a dense-compact matrix and contained less unreacted raw materials. Further, a higher reaction of Si-Al in the geopolymerization process produced aluminosilicate and in addition, the preparation of the geopolymers in a hot mixture (produced an exothermic from sodium silicate and sodium hydroxide into water) in this study may have also contributed to the compressive strength. However, different MK's from other locations may need different ratios and particle sizes to achieve high compressive strength.

Acknowledgement

The authors gratefully acknowledge the financial support of the Office of the Higher Education Commission and thesis research funding from Prince of Songkla University, Thailand, as well as the use of the facilities of the Department of Mining and Materials Engineering and Department of Civil Engineering, Prince of Songkla University.

REFERENCES

1. Bakharev T.: Cem. & Concr. Res. *35*, 658 (2005).
2. Duxson P., Provis J.L., Lukey G.C.: Cem. & Concr. Res. *37*, 1590 (2007).
3. Elimbi A., Tchakoute H.K., Njopwouo D.: Contr. & Build. Mater. *25*, 2805 (2011).
4. Nazari A., Bagheri A., Riahi S.: Mater. Sci. and Eng. A *528*, 7395 (2011).
5. Mohsen Q., Mostafa N.Y.: J. Ceram. *54*, 160 (2010).
6. Allahverdi A., Nani E.N.,Yazdanipour M.: J. Ceram. *55*, 68 (2011)
7. Al Bakri A.M.M., Kamarudin H., Bnhussian M., 7. Rafiza A.R., Zarina Y.: ACI Mater. J., *109*, 503 (2012).
8. Office of Agricultural Economics. www.oae.go.th, (2012).
9. Dalimin M.N.: Malaysia, Renewable Energy *6*, 435 (1995).
10. Sata V., Jaturapitakkul C., Kiattikomaol K.: J. Mater. Civ. Eng. *16*, 623 (2004).
11. ASTM 109/C109M-98, "*Test Method for Compressive Strength of Hydraulic Cement Mortar (Using 2-in. or [50-mm] Cube Specimens)"* (1998).
12. ASTM C596-96, "*Test Method for Drying Shrinkage of Mortar Containing Portland Cement"* (1996).
13. ASTM C490-96, *"Practice for Use of Apparatus for the Determination of Length Change of Hardened Cement Paste, Mortar, and Concrete"* (1996).
14. Rovnanik P.: Contr. & Build. Mater. *24*, 1176 (2010).
15. Silva P.D., Sagoe-Crenstil K., Sirivivatnanon V.: Cem. & Concr. Res. *37*, 512 (2007).
16. Silva P.D., Sagoe-Crenstil K.: Cem. & Concr. Res. *38*, 870 (2008).
17. Chindaprasirt P., Silva P.D., Sagoe-Crentsil K., Hanjitsuwan S.: J. Mater. Sci. *47*, 4876 (2012).
18. Alvarez-Ayuso E., Querol X., Plan F., Alastuey A., Moreno N., Izquierdo M., Font O., Moreno T., Diez S., Vazquez E., Barra M.: J. Hazard. Mater. *154*, 175 (2008).
19. Temuujin J., Riessen A.V., Williams R.: J. Hazard. Mater. *167*, 82 (2009).
20. van Jaarsveld J.G.J., van Deventer J.S.J., Lukey G.C. Mater. Lett. *57*, 1272 (2003).
21. Chun Y.Y., Sharifah A.S.A.K., Ying P.L., Sharifah N.S.A., Zurinawati Z.: Fuel Pro. Tech. *89*, 693 (2008).
22. Granizo M.L., Blanco-Varela M.T., Martenes-Ramirez S.: J. Mater. Sci. *42*, 2934 (2007).
23. Hongling W., Haihong L. Fengyuan Y.: Coll. and Surf. A. *268*, 1 (2005).
24. Ismail I., Bernal S.A., Provis J.L., Hamdan S., van Deventer J.S.J.: Mater. and Struct. *46*, 361 (2013).